
Appendix A. Electronic Supplementary Material

Multifunctional buried interface modification for efficient and stable SnO₂-based perovskite solar cells

Rui Wu,^a Junhua Meng,^{*a} Yiming Shi,^a Zhengchang Xia,^{b,c} Chunxia Yan,^a Lisheng Zhang,^a Wenkang Liu,^a Jinliang Zhao,^a Jinxiang Deng^a and Xingwang Zhang^{b,c}

^a School of Physics and Optoelectronic Engineering, Beijing University of Technology, Beijing 100124, P. R. China E-mail: jhmeng@bjut.edu.cn

^b Key Lab of Semiconductor Materials Science, Institute of Semiconductors, Chinese Academy of Sciences, Beijing 100083, P. R. China

^c Center of Materials Science and Optoelectronics Engineering, University of Chinese Academy of Sciences, Beijing 100049, P. R. China

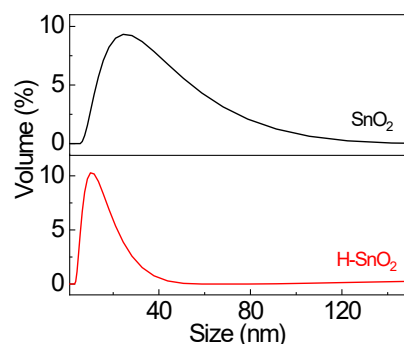


Fig. S1. DLS measurements of the dispersion of pristine SnO₂ and H-SnO₂.

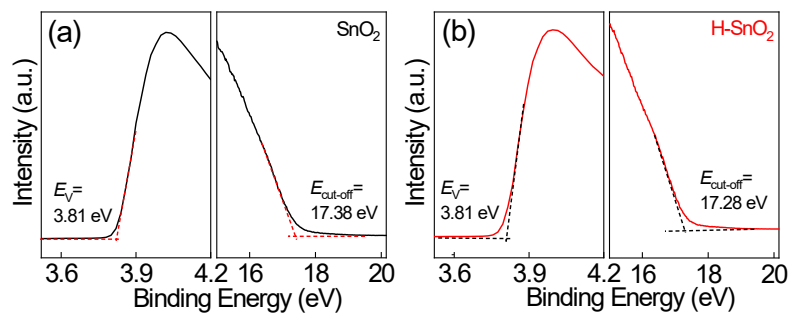


Fig. S2. The UPS spectra of (a) pristine SnO₂ and (b) H-SnO₂ film, where the secondary electron cutoff and the Fermi edge are focused.

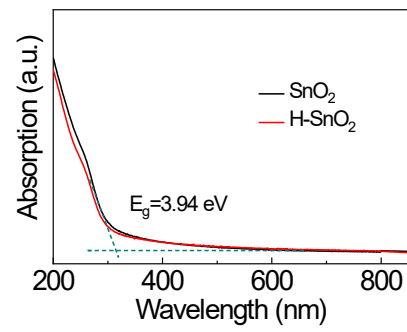


Fig. S3. The UV-vis absorption spectra of the pristine SnO_2 and H- SnO_2 film, from which the bandgap of the samples is estimated to be 3.94 eV.

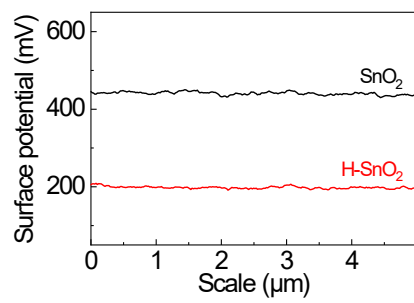


Fig. S4. The surface potential profiles of the pristine SnO₂ and H-SnO₂ films taken at the positions marked by white line in the KPFM images (Fig. 1e and 1f).

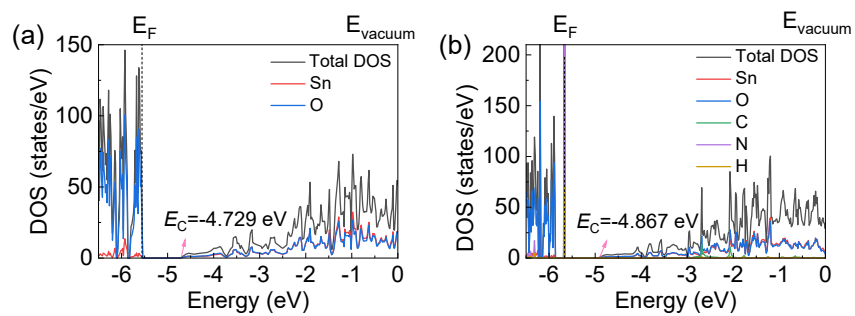


Fig. S5. Electronic DOS of (a) SnO_2 , (b) H-SnO_2 .

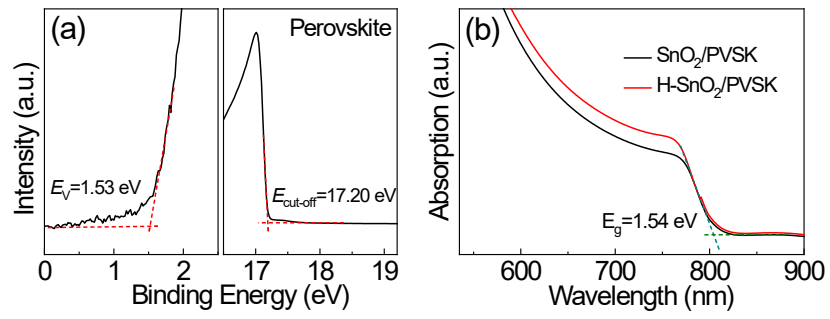


Fig. S6. (a) The UPS spectra of perovskite film, (b) UV-vis absorption spectra of the perovskite films deposited on SnO_2 ETLs.

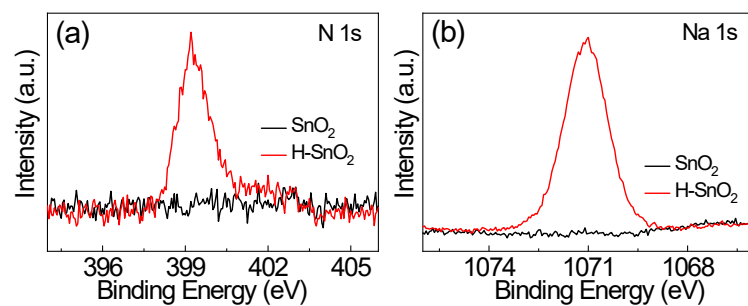


Fig. S7. XPS core-level spectra of (a) N 1s and (b) Na 1s for SnO₂ and H-SnO₂ film.

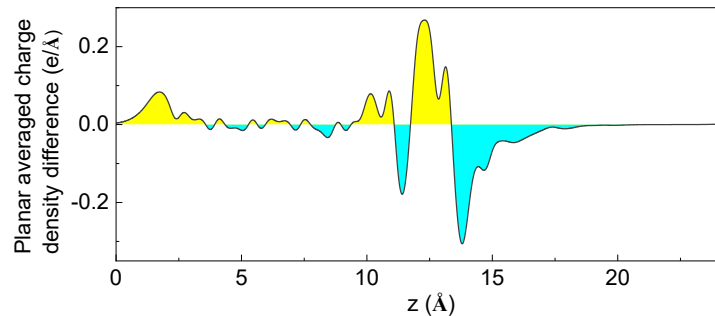


Fig. S8. Plane-averaged charge density difference of $\text{SnO}_2/\text{HEDTA}$ interface, the cyan and yellow regions correspond to the charge depletion and accumulation regions, respectively.

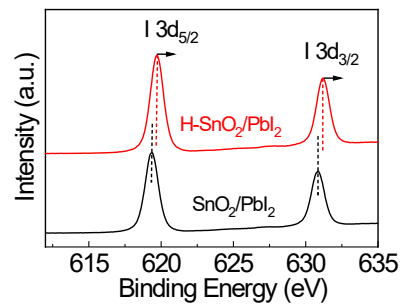


Fig. S9. I 3d core-level spectra for the PbI₂ films coated on SnO₂ and H-SnO₂ ETLs.

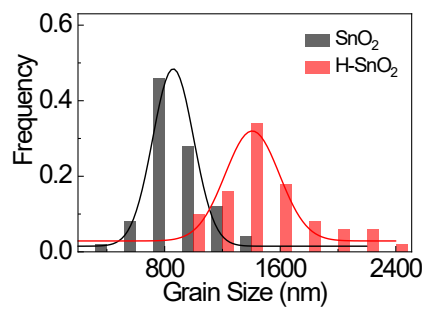


Fig. S10. The grain size distribution diagram of perovskite films coated on SnO_2 and H-SnO_2 ETLs.

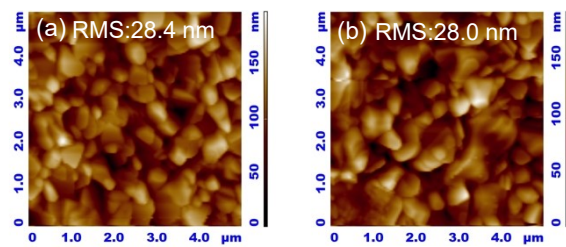


Fig. S11. AFM images of perovskite films deposited on (a) SnO_2 and (b) H-SnO_2 , the scan area is $5 \times 5 \mu\text{m}^2$.

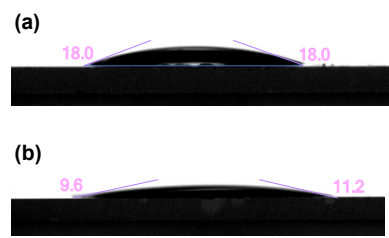


Fig. S12. Contact angle measurements of DMF on (a) SnO_2 and (b) H- SnO_2 film.

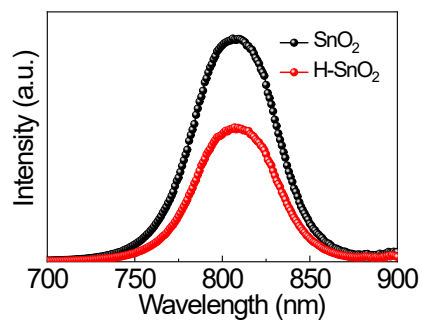


Fig. S13. Steady-state PL spectra of the perovskite films deposited on the SnO_2 and H- SnO_2 substrates.

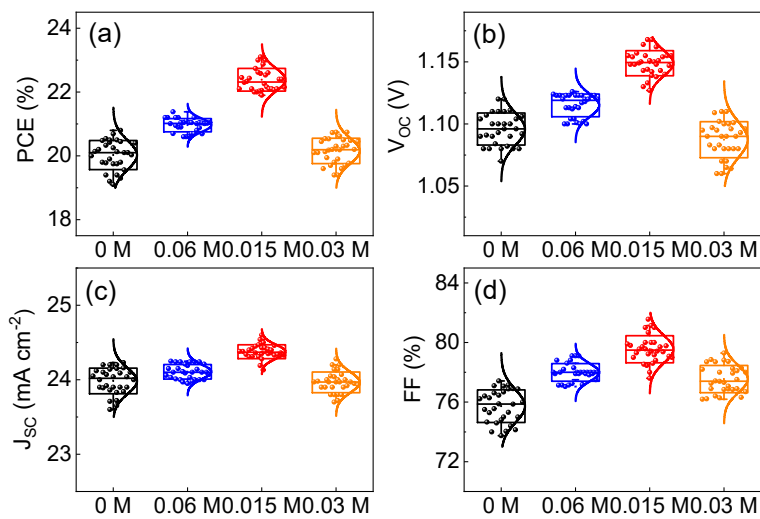


Fig. S14. Statistic diagram of (a) PCE, (b) V_{oc}, (c) J_{sc} and (d) FF for the PSCs based on SnO₂ ETL with different concentration of HEDTA-3Na. The statistical data were collected from 30 cells for each concentration.

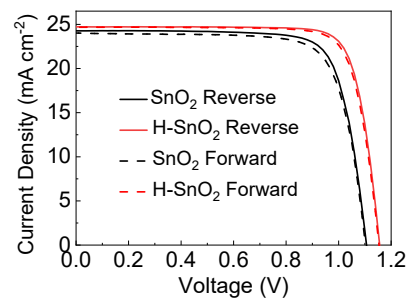


Fig. S15. *J-V* curves measured by the reverse scan and forward scan of the PSCs based on pristine SnO₂ and H-SnO₂ ETLs, the photovoltaic parameters are listed in [Table S2](#).

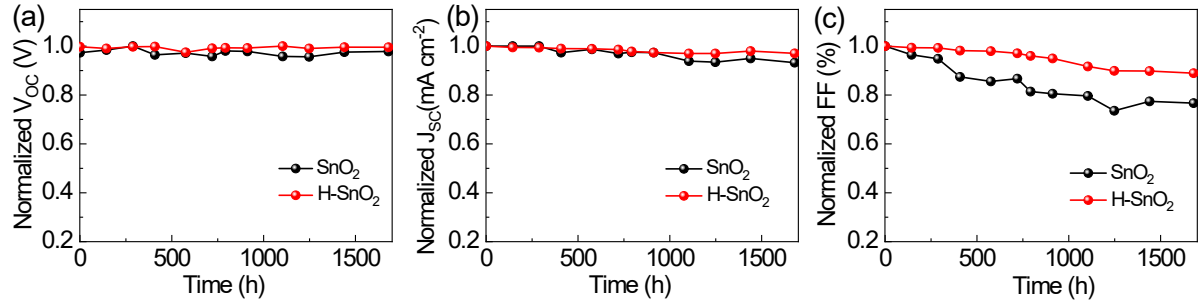


Fig. S16. Long-term stability of (a) V_{OC} , (b) J_{SC} and (c) FF (unencapsulated devices) for the PSCs with SnO_2 and H-SnO_2 ETLs.

Table S1. The TRPL spectra parameters of perovskite based on SnO₂ and H-SnO₂ ETLs.

Samples	A ₁ (%)	τ ₁ (ns)	A ₂ (%)	τ ₂ (ns)	τ _{ave} (ns)
SnO ₂	85.6	79.2	14.4	383	215.5
H-SnO ₂	85.2	46.8	14.8	183.3	101.8

Table S2. Photovoltaic parameters for PSCs made with SnO₂ or H-SnO₂ under reverse and forward scan directions.

Samples	Scan direction	V _{OC} (V)	J _{SC} (mA cm ⁻²)	FF (%)	PCE (%)	HI
SnO ₂	Reverse	1.106	24.26	77.57	20.82	0.032
	Forward	1.102	24.01	76.13	20.16	
H-SnO ₂	Reverse	1.156	24.72	80.86	23.11	0.014
	Forward	1.154	24.67	80.02	22.78	

Table S3. EIS parameters of devices based on SnO₂ and H-SnO₂ ETLs.

Sample	R _{tr} (Ω)	R _{rec} (Ω)
SnO ₂	580.6	3172
H-SnO ₂	317.2	6021